Proc. SY.RO.CO'94, IFAC. 1994. Vol. 2, pp. 389-394.

DECENTRALIZED IMPEDANCE CONTROL

M. DOYON*, **V. HAYWARD*** and **M. PELLETIER****

**McGill University, Centre for Intelligent Machines, Montréal, Québec, CANADA, H3A 2A7*

***Institut de recherche d'Hydro-Québec, Varennes, Québec, CANADA, J3X 1S1*

Abstract. We describe an impedance control method following an independent joint control approach. Simple impedance controllers are set up at each joint and coupling among the joints is cancelled using equally simple compensators. It is possible to program any diagonal visco-elastic impedance matrix in Cartesian task coordinates within the limits of what can be achieved at the joint level. The performance depends on the precise tracking of joint torque specifications which may be achieved by minor feedback loops and co-located joint torque sensors. This technique takes advantage of the frequency separation of signals describing the dynamics of most serial robot manipulators to achieve excellent performance and robustness at a low computational cost. In the described method, we should more appropriately speak of *control of the impedance* rather than of impedance control. Experimental results are reported using a Sarcos redundant manipulator model GRLA (General Robotic Large Arm). The method applies equally well to kinematically non-redundant and redundant manipulators.

Key Words: Decentralized control; Decoupling; Control of impedance

1. INTRODUCTION

Many applications of robot manipulators to date have been based on position control, but when a robot manipulator makes contact with the environment, the control of both force and motion is required. One approach is "impedance control": the robot is controlled to approximate as a mass-spring-damper system whose parameters can be specified arbitrarily (Hogan, 1985). Impedance control requires force sensing devices to improve performance because friction and actuator dynamics are typically the dominating dynamical effects when a manipulator is made to "comply" with an environment at low velocity.

It is natural to use Cartesian task coordinates to perform the control of impedance. In recent years, a number of impedance control schemes have been proposed based on using feedback from a force sensor interposed between the arm proper and an end-effector, see for example (Lawrence, 1988). The implementation proposed here requires instead co-located joint torque sensors. Co-located torque sensors allow a larger bandwidth and control robustness since the feedback does not include the structural dynamics of the arm. Only an approximate knowledge of the dynamics of the robot is needed to achieve good results (Wu and Paul, 1980; An and Hollerbach, 1987; Eppinger and Seering, 1987) and no coodinates transformations are needed in the feedback loop.

Salisbury first proposed the idea of an active stiffness controller, mapping Cartesian stiffness expressed in task coordinates into joint coordinates stiffness (Salisbury, 1980). In this paper, a generalization of this idea is proposed by adding an active damping controller and eventually an active inertia compensator. In this approach, a collection simple SISO controllers and decoupling compensators are needed and the computations can be performed on the basis of one computing unit (CPU of task) per joint.

2. DECENTRALIZED IMPEDANCE CONTROL

2.1. *Basic principle*

The manipulator is to be controlled to appear like a second order linear system (mass-spring-damper system) to an external observer in Cartesian coordinates. A desired Cartesian coordinates impedance is derived for the joint coordinates control law as follows. We first map the Cartesian coordinates into joint coordinates. Assuming small displacements we linearize to obtain:

$$\tau = J^T F \quad (1)$$
$$X \approx J\theta \quad (2)$$

then, in the Laplace domain,

$$F(s) = Z_c(s)X(s) \quad (3)$$
$$\tau(s) = Z_\theta(s)\theta(s) \quad (4)$$

Proc. SY.RO.CO'94, IFAC. 1994. Vol. 2, pp. 389-394.

thus

$$Z_\theta(s) = J^T Z_c(s) J \qquad (5)$$

where $Z_c(s) = B_x s + K_x$

This method for computing the nominal impedance of each joint has the advantage that it does not require a Jacobian inversion, reducing the computations and alleviating problems near singularities. There is however no reason why the resulting $Z_\theta(s)$ should be diagonal (and not necessarily positive definite) when $Z_c(s)$ is chosen to be diagonal, except in special cases.

Conversely, a diagonal $Z_\theta(s)$ (namely PD control) will not lead to $Z_c(s)$ diagonal, meaning that cross coupling occurs in Cartesian space. When $Z_c(s)$ is diagonal, $Z_\theta(s)$ is symmetric and the terms outside the diagonal (cross coupling terms) are *not* negligible. However, in general the diagonality or degree of decoupling of $Z_\theta(s)$ will vary with the robot configuration. A non diagonal $Z_\theta(s)$ means that the errors in one joint will affect the commanded torque in all the other joints (see equation 4) as was pointed out in (Salisbury, 1980) . Only certain cases will lead to decoupling which is an architectural kinematic property of the underlying mechanism as shown in (Hayward, 1993).

Redundancy may contribute to reduce or even cancel cross coupling terms by using the additional degrees of freedom to select a configuration which minimizes the off diagonal terms of the joint space impedance matrix for a given Cartesian coordinates impedance matrix. The relationship between p, the number of parameters to control in joint space and N, the number of degrees of freedom is given by:

$$p = \sum_{i=0}^{N-1} (-1)^i \, (N-i)^2 \qquad (6)$$

For purposes of illustration, the case of a planar robot with three DOF is now discussed. It is possible to configure a manipulator of this kind to produce a given diagonal Cartesian coordinates impedance matrix from a diagonal joint space impedance matrix. A Cartesian coordinates impedance matrix specifies three terms, the impedance in the x and y directions and the cross coupling term between x and y fixed to zero, ideally. Since the robot has three joints it can be verified that there is a unique solution to three equations with three unknowns. Redundancy can be used to yield a diagonal joint space matrix that will satisfy the Cartesian specifications.

In the more general case of a seven degree of freedom robot, from equation 6, we find that 28 parameters are to be determined, among which 21 must be set to zero. A manipulator with at least 28 degrees of freedom would be capable of yielding a diagonal Cartesian coordinates impedance matrix from a diagonal joint space impedance matrix. Redundancy, in this case, can only contribute to minimize the cross coupling terms. Therefore, an optimization method can be applied to find postures that minimize the coupling but decoupling cannot occur in general.

If one decides to set the diagonal terms of $Z_\theta(s)$ by means of feedback control, the corresponding joint controllers are PD controllers whose gains are scheduled or continuously modified as the task progresses. With the off diagonal terms neglected, the system will be highly coupled but the control is quite robust. From equation 4, the torque command to one joint is given by:

$$\tau_i = \sum_{j=1}^{N} Z_{i,j}\theta_j \qquad (7)$$

$$\tau_i = Z_{i,i}\theta_i + \sum_{j=1, j\neq i}^{N} Z_{i,j}\theta_j \qquad (8)$$

Next, we look at the off diagonal terms of Z for each actuator to apply compensating torques (second right hand side term of equation 8) calculated from the position of the other joints. The resulting impedance matrix in Cartesian coordinates is then decoupled as will be presented in section (5).

3. JOINT SPACE IMPEDANCE CONTROLLER

While the decentralized impedance control operates in the joint space, it is important to derive the Cartesian space transfer function. The transfer function will be obtained by mapping the joint space control system into a Cartesian coordinates. It is well shown that the joint coordinates dynamics: inertia, damping and stiffness are captured by,

$$\tau_{robot} = D_\theta \ddot{\theta} + V(\theta, \dot{\theta}) + G(\theta) \qquad (9)$$

Then the desired impedance expressed in joint coordinates is,

$$\begin{aligned} \tau_{robot} &= M_\theta(\ddot{\theta}_d - \ddot{\theta}) + B_\theta(\dot{\theta}_d - \dot{\theta}) \\ &+ K_\theta(\theta_d - \theta) + \hat{V}(\theta, \dot{\theta}) + \hat{G}(\theta) \qquad (10) \end{aligned}$$

Joining equations 9 and 10,

$$\begin{aligned} D_\theta \ddot{\theta} + V(\theta, \dot{\theta}) + G(\theta) &= M_\theta(\ddot{\theta}_d - \ddot{\theta}) \\ &+ B_\theta(\dot{\theta}_d - \dot{\theta}) + K_\theta(\theta_d - \theta) \\ &+ \hat{V}(\theta, \dot{\theta}) + \hat{G}(\theta) \qquad (11) \end{aligned}$$

Proc. SY.RO.CO'94, IFAC. 1994. Vol. 2, pp. 389-394.

assuming,

$$\begin{aligned} \tau_d &= M_\theta \ddot{\theta}_d + B_\theta \dot{\theta}_d + K_\theta \theta_d & (12) \\ \tau &= J^T F & (13) \\ \delta x &\approx J \delta \theta & (14) \\ \ddot{x} &= J\ddot{\theta} + \dot{J}\dot{\theta} & (15) \end{aligned}$$

we have,

$$\begin{aligned} F_d = \; & J^{-T}(M_\theta + D_\theta)\ddot{\theta} + J^{-T} B_\theta \dot{\theta} + \\ & J^{-T} K_\theta \theta + J^{-T}(V - \hat{V}) + \\ & J^{-T}(G - \hat{G}) \qquad (16) \end{aligned}$$

replacing equation 14 in equation 16,

$$\begin{aligned} F_d = J^{-T}(M_\theta + D_\theta)J^{-1}\ddot{x} + J^{-T} B_\theta J^{-1}\dot{x} \\ + J^{-T} K_\theta J^{-1} x + J^{-T}(V - \hat{V}) \\ + J^{-T}(G - \hat{G}) - J^{-T}(M_\theta + D_\theta)J^{-1}\dot{J}\dot{\theta} \quad (17) \end{aligned}$$

where

$$\begin{aligned} M_\theta &= J^T M_x J & (18) \\ B_\theta &= J^T B_x J & (19) \\ K_\theta &= J^T K_x J & (20) \\ \mathcal{D} &= J^{-T} D_\theta J^{-1} & (21) \end{aligned}$$

so that,

$$F_d = ((\mathcal{D} + M_x)s^2 + B_x s + K_x)x + \Delta \quad (22)$$

$$\begin{aligned} \Delta = \; & J^{-T}(V - \hat{V}) + J^{-T}(G - \hat{G}) - \\ & J^{-T}(M_\theta + D_\theta)J^{-1}\dot{J}\dot{\theta} \qquad (23) \end{aligned}$$

At relatively low speed, the centrifugal and coriolis term becomes negligible and so does the rate of change of the Jacobian matrix. The error due to gravity subsists and depends on the precision of the compensation. Assuming perfect compensation, the transfer function becomes,

$$\frac{x}{F_d} = ((\mathcal{D} + M_x)s^2 + B_x s + K_x)^{-1} \quad (24)$$

Notice that the robot inertia appears in equation 24. Since this matrix is not diagonal it will cause errors in the transient response. These can be minimized using redundancy of the manipulator when possible.

An example using a 2 DOF robot is now worked out to gain some insight on the control algorithm.

In the following, we assume that each link of actuator can be modeled with a torque source acting on a simple inertia. The controller used in the experiments has in fact an internal force loop with enough gain make this simplification valid. Figure 1 shows the basic joint control scheme. Since we assume for now small displacements and low velocities, only the moments of inertia are considered and the products of inertia are neglected.

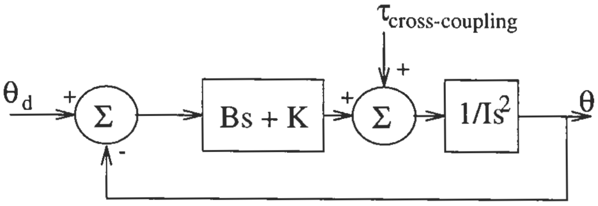

Fig. 1. Basic joint control scheme

The desired joint impedances are computed from equation 5. A decoupling compensator is introduced to cancel cross coupling terms by adding an equivalent joint torque (figure 2). The cross coupling torque for a particular actuator is given by:

$$\tau_i = \sum_{j=1, j \neq i}^{N} Z_{i,j} \theta_j \quad (25)$$

Given a desired Cartesian coordinates impedance,

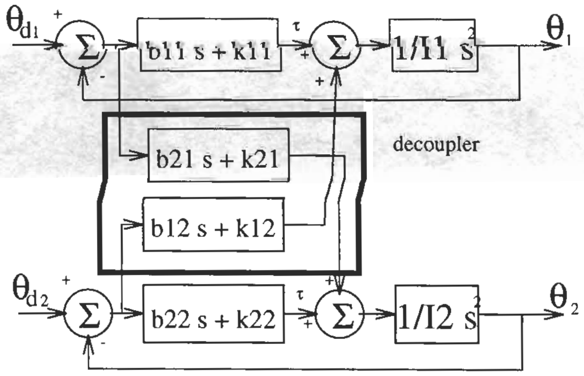

Fig. 2. 2 D.O.F. decentralized impedance controller

the joint impedances can be computed using the corresponding Jacobian matrix:

$$Z_c(s) = \begin{pmatrix} b_x s + kx & 0 \\ 0 & b_y s + k_y \end{pmatrix} \quad (26)$$

$$Z_\theta = \begin{pmatrix} z_{11} & z_{12} \\ z_{21} & z_{22} \end{pmatrix}$$

$$= \begin{pmatrix} j_{11}^2 z_x + j_{21}^2 z_y & j_{11} j_{12} z_x + j_{21} j_{22} z_y \\ j_{11} j_{12} z_x + j_{21} j_{22} z_y & j_{12}^2 z_x + j_{22}^2 z_y \end{pmatrix}$$

Assuming small displacement, we have

$$\theta = A^{-1}\tau \quad (27)$$

where A is the matrix containing the transfer function, relating θ_i to τ_j (i,j = 1 to N), obtained from

Proc. SY.RO.CO'94, IFAC. 1994. Vol. 2, pp. 389-394.

figure (2).

$$\begin{aligned} t_{11} &= (i_1 s^2 + b_{11}s + k_{11}) \\ t_{22} &= (i_2 s^2 + b_{22}s + k_{22}) \\ t_{12} &= (b_{12}s + k_{12}) \\ t_{21} &= (b_{21}s + k_{21}) \end{aligned}$$

$$A = \begin{pmatrix} t_{11} & t_{12} \\ t_{21} & t_{22} \end{pmatrix} \quad (28)$$

$$X = \frac{JA^{-1}J^T F}{t_1 t_2 - t_{12}t_{21}} \quad (29)$$

The pattern in the algebraic structure of the denominator of the transfer function can be roughly described as the product of the denominators of each joint's transfer function minus a correction term.

$$\text{denominator} = \prod_{i=1}^{N}(I_i s^2 + b_{ii}s + k_{ii}) - \textit{decoupler correction} \quad (30)$$

The complexity of this term increases with the number of DOF. It has the form of multiple combinations of each decoupler terms times the *diagonal* terms $(I_i s^2 + b_{ii}s + k_{ii})$. Since the b_{ij} and k_{ij} are functions of b_x,b_y,k_x,k_y, we can simplify further to obtain an expression in Cartesian coordinates:

$$\begin{aligned} \text{Den} &= as^4 + (b_1 B_x + b_2 B_y)s^3 + \\ &\quad (b_1 K_x + b_2 K_y + cB_x B_y)s^2 + \\ &\quad c(K_x B_y + K_y B_x)s + cK_x K_y \quad (31) \\ \frac{\Delta x}{\Delta F_x} &= \frac{b_1 s^2 + cB_y s + cK_y}{Den} \quad (32) \\ \frac{\Delta x}{\Delta F_y} &= \frac{ds^2}{Den} \quad (33) \\ \frac{\Delta y}{\Delta F_x} &= \frac{\Delta x}{\Delta F_y} \quad (34) \\ \frac{\Delta y}{\Delta F_y} &= \frac{b_2 s^2 + cB_x s + cK_x}{Den} \quad (35) \end{aligned}$$

where

$$\begin{aligned} a &= I_1 I_2 \\ b_1 &= (I_1 j_{12}^2 + I_2 j_{11}^2) \\ b_2 &= (I_1 j_{22}^2 + I_2 j_{21}^2) \\ c &= (j_{11}j_{22} - j_{12}j_{21})^2 \\ d &= (I_1 j_{12} j_{22} + I_2 j_{11} j_{21}) \end{aligned}$$

It is readily seen that there is no steady state error to a step input since:

$$\lim_{s\to 0}\frac{\Delta x}{\Delta F_x} = \frac{1}{k_x}, \quad \lim_{s\to 0}\frac{\Delta y}{\Delta F_y} = \frac{1}{k_y} \quad (36)$$

and

$$\lim_{s\to 0}\frac{\Delta x}{\Delta F_y} = \frac{\Delta y}{\Delta F_x} = 0 \quad (37)$$

If no decoupler is used, then the final value will depend on the configuration of the robot as well as the Cartesian coordinates stiffness matrix. Obviously, the Cartesian coordinates system will be coupled.

4. STIFFNESS ERROR

So far, we assumed small displacements and a linearization was performed to map the Cartesian space position into joint space angles. As the robot is moved away from its nominal position the linearization no longer is valid. The error resulting from this linearization varies depending on the robot configuration. We have,

$$\begin{aligned} \varepsilon &= \frac{J\Delta\theta - (\Lambda(\theta) - \Lambda(\theta_d))}{(\Lambda(\theta) - \Lambda(\theta_d))} \quad (38) \\ K_{effective} &= K_{desired}\frac{J\Delta\theta}{(\Lambda(\theta) - \Lambda(\theta_d))} \quad (39) \end{aligned}$$

given that the Cartesian displacement, $(\Lambda(\theta) - \Lambda(\theta_d))$, is different of zero.

When Δx is large, the error arises from the approximation:

$$\Delta x \approx J\Delta\theta \quad (40)$$

To correct this error, an incremental update of the desired joint space position is performed,

$$\theta_{dnew} = \theta + J^{-1}\Delta x \quad (41)$$

In the case of redundant manipulators, an additional constraint can always be added leading to a square Jacobian matrix which is invertible.

5. EXPERIMENTAL RESULTS

A 7 DOF manipulator (Sarcos GRLA arm) located at Institut de recherche d'Hydro-Québec for which the last three articulations (the wrist) were locked was used for experimentation. Each actuator torque is regulated via an analog PD controller.

The cross-coupling terms are computed digitally

Proc. SY.RO.CO'94, IFAC. 1994. Vol. 2, pp. 389-394.

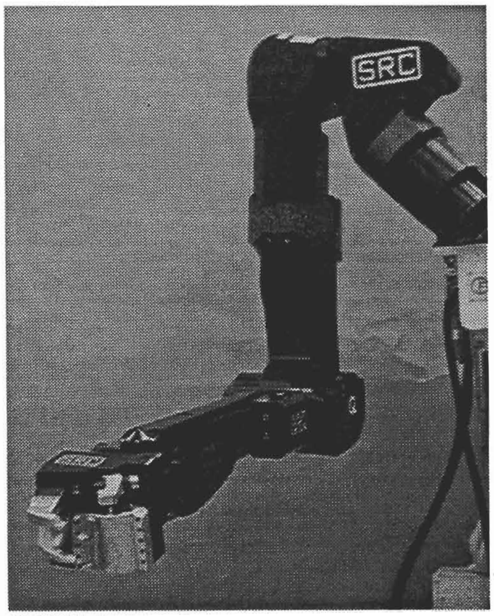

Fig. 3. Sarcos Arm (General Robotic Large Arm)

and the diagonal terms are set by analog PD controllers. This implementation increases the robustness and the stability of the controller since it reduces the problems due to sampling and delay in conventional digital controllers and allows the cross-coupling correction to be performed at a relatively low sampling frequency. A rate of 100 Hz is perfectly satisfactory since the position and velocity signals occur in a rather low frequency band.

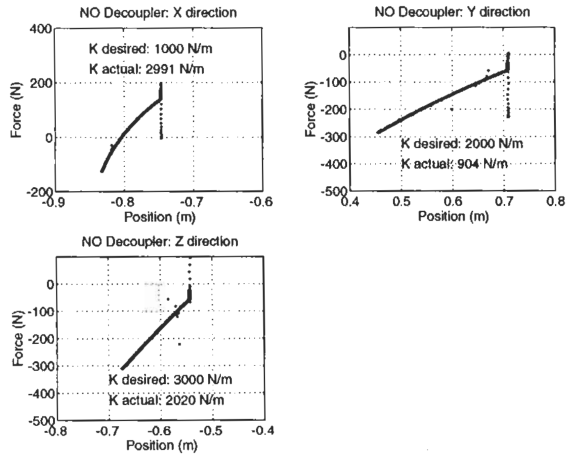

Fig. 4. No decoupler: Force vs Displacement

Two experiments have been carried out. The first one consists of programming the Cartesian coordinates stiffness ($F = KX$) and then to compare the static case responses with and without decoupler. An external force causing a deflection of the end-effector from its desired position is applied. A decoupler, as seen on figure 5, ensures no error on the desired stiffness in all directions. In figure 4 no decoupler is used and the error is quite large.

In a second experiment, the complete controller (with decoupler) is used and the dynamic response is studied. The proposed controller does not require the calculation of a dynamic model, but the modification of the dynamic response require the knowledge of the inertia matrix. The joint coordinates inertia matrix has been approximated and then is mapped into Cartesian coordinates. Given the mass estimate, the desired damping and stiffness in Cartesian coordinates, a theoretical step response in the x direction has been computed and compared to experimental data. The result is presented in figures 6 and 7. Those figures also show the dynamic coupling between the y and z directions. As seen on figure 5 showing a cloud of

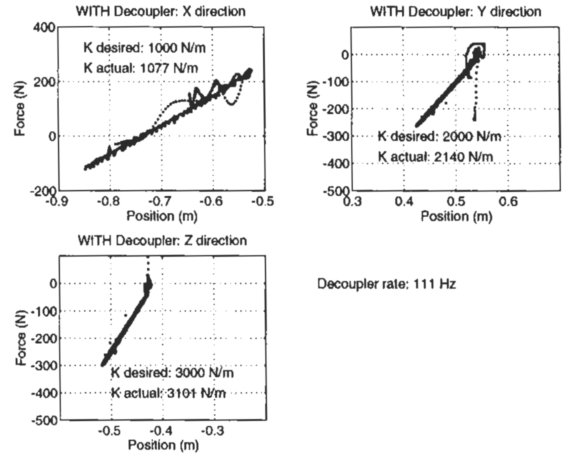

Fig. 5. With Decoupler: Force vs Displacement

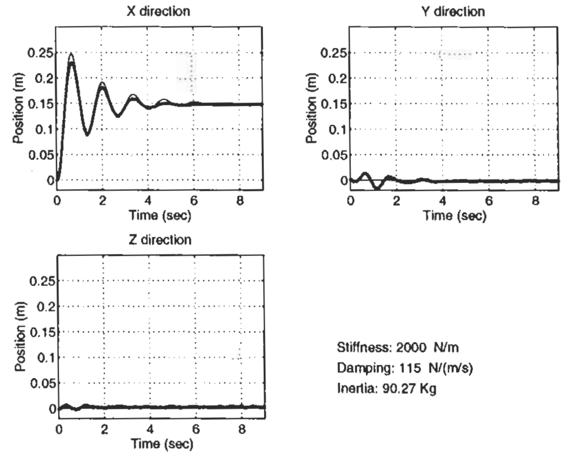

Fig. 6. With Decoupler: Dynamic Response

points, the relationship between the applied force and the displacement is linear. When no decoupler is present, the effective stiffness can be quite far from the desired stiffness. Activating the decoupler leads to a much more accurate effective stiffness.

Proc. SY.RO.CO'94, IFAC. 1994. Vol. 2, pp. 389-394.

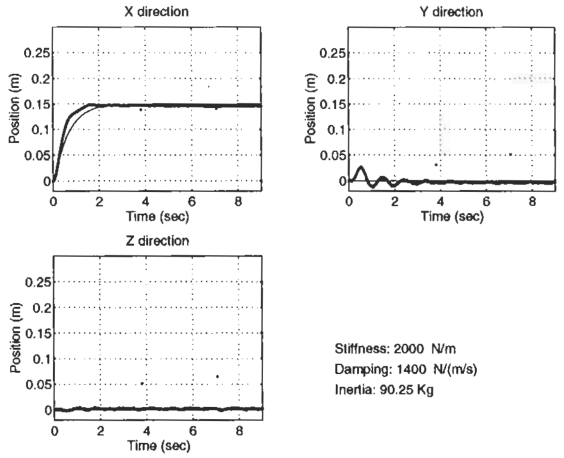

Fig. 7. With Decoupler: Dynamic Response

6. CONCLUSION

We presented a method to program a desired Cartesian impedance on a robot manipulator. We gave an expression for the Cartesian coordinates transfer function and showed that this method could be easily implemented.

7. ACKNOWLEDGEMENTS

The financial support for this work has been provided by the Natural Sciences and Engineering Research Council of Canada (NSERC) and also by the Institut de recherche d'Hydro-Québec (IREQ). The authors would also like to acknowledge the support and help of Martin Boyer and Pierre Girard of IREQ. Additional support was provided by IRIS, the Institute for Robotics and Intelligent Systems part of Canada's National Centers of Excellence program (NCE) in the form of related projects.

8. REFERENCES

An, C.H. and Hollerbach, J.M. (1987). Dynamic stability issues in force control manipulators. *Proceedings of the IEEE International Conference on Robotics and Automation* pp. 890–896.

Eppinger, S.D. and Seering, W.P. (1987). Understanding bandwidth limitations in robot force control. *Proceedings of the IEEE International Conference on Robotics and Automation* pp. 904–909.

Eppinger, S.D. and Seering, W.P. (1989). Three problems in robot force control. *Proceedings of the IEEE International Conference on Robotics and Automation* pp. 392–397.

Hayward V., Nemri C., Chen X. and Duplat B. (1993). Hand controller based on parallel mechanism with decoupled stiffness. *International JournaL of Robotics Systems* **10**(5), 767–790.

Hogan, N. (1985). Impedance control: An approach to manipulation (parts I ,II ,III). *ASME Journal of Dynamic Systems, Measurements and Control* **107**, 1–24.

Iwaki, S. and Matsuo S. (1990). A new approach to compliance control of robot manipulators using stable negative compliance. *Nippon Telegraph and Telephone Corporation* pp. 145–156.

Kaneko M., Inamura N., Yokoi K. and Tanie K. (1988). Direct compliance control of manipulator arms - basic concept and application examples. *Proceedings of IFAC Symposium on Robot Control* pp. 8.1–8.6.

Lawrence, D. (1988). Impedance control stability properties in common implementations. *Proceedings of the IEEE International Conference on Robotics and Automation* pp. 1185–1190.

Salisbury, J.K. (1980). Active stiffness control of a manipulator in cartesian coordinates. *Proceedings of the 19th IEEE Conference on Decision and Control* pp. 95–100.

Tanie K., Yokoi K. and Kaneko M. (1990). Compliance control with considerations of trajectory control charateritics. *AIST-MITI* pp. 275–280.

Wu, C. and Paul R.P. (1980). Manipulator compliance based on joint torque control. *Proceedings of the 19th IEEE Conference on Decision and Control* pp. 88–94.